THE JOURNAL OF PHYSICAL CHEMISTRY B

ARTICLE

pubs.acs.org/JPCB

Theoretical Study of the Electronic−Vibrational Coupling in the Q_y States of the Photosynthetic Reaction Center in Purple Bacteria

Yuanyuan Jing, Renhui Zheng, Hui-Xue Li, and Qiang Shi*

Beijing National Laboratory for Molecular Sciences, State Key Laboratory for Structural Chemistry of Unstable and Stable Species, Institute of Chemistry, Chinese Academy of Sciences, Zhongguancun, Beijing 100190, China

ABSTRACT: Inspired by the recent observation of correlated excitation energy fluctuations of neighboring chromophores (Lee et al. *Science* **2007**, *316*, 1462), quantum chemistry calculations and molecular dynamics simulations were employed to calculate the electronic−vibrational coupling in the excited states of the photosynthetic reaction center of purple bacteria *Rhodobacter* (*Rb.*) *sphaeroides*. The ground states and lowest excited (Q_y) states of isolated bacteriochlorophyll a (BChl *a*) and bacteriopheophytin (BPhe) molecules were first optimized using density functional theory (DFT) and time-dependent density functional theory (TDDFT). Normal mode analyses were then performed to calculate the Huang−Rhys factors of the intramolecular vibrational modes. To account for intermolecular electronic−vibrational coupling, molecular dynamics simulations were first performed. The ZINDO/S method and partial charge coupling method were then used to calculate the excitation energy fluctuations caused by the protein environment and obtain the spectral density. No obvious correlations in transition energy fluctuations between BChl *a* and BPhe pigments were observed in the time scale of our MD simulation. Finally, by comparing the calculated absorption spectra with experimental ones, magnitudes of inhomogeneous broadening due to the static disorder were estimated. The large amplitude of the static disorder indicates that a large portion of the spectral density and their correlations may still be hidden in the inhomogeneous broadening due to the finite MD simulation time.

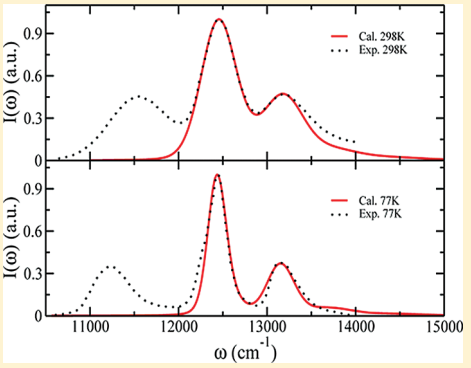

I. INTRODUCTION

Photosynthesis is by far the most important process in transforming energy from solar radiation into chemical energy for life on Earth.[1,2] It is of no doubt that a complete understanding of the molecular mechanisms of photosynthesis would provide invaluable insights into finding cheap and efficient ways for solar energy harvesting. The initial steps of charge separation in photosynthetic organisms occur in a pigment−protein complex called the reaction center (RC), which has received intensive research interest over the past decades.[3−7] The RC of purple bacteria *Rhodobacter* (*Rb.*) *sphaeroides* contains three protein subunits (L, M, and H), four bacteriochlorophyll a (BChl *a*) molecules, two bateriopheophytins (BPhe), two quinones, a nonheme iron, and a carotenoid.[8] The photoinduced electron transfer process is initialized by a charge-separation process transferring an electron from the photoexcited special pair (P) to BPhe (H) via BChl *a* (B) within about 3 ps.[7,9]

The RC has also served as a model system to study the effect of protein environments on spectra and energy transfer dynamics.[6,10−12] The absorption spectra of the RC of *Rb. sphaeroides* show three peaks between 700 and 950 nm, which have been assigned to the Q_y transitions of the P (870 nm), B (800 nm), and H (760 nm) pigments.[13] Experimentally, the hole-burning spectra,[14,15] resonance Raman spectra,[13,16] and fluorescence line narrowing (FLN)[17,18] have revealed that the Q_y electronic transitions are coupled to several vibrational modes. Vibrational modes were also found to be responsible for the quantum beats in the pump−probe spectra.[19] Such electronic−vibrational couplings were found to play an important role in determining the spectra,[20−22] as well as charge transfer[15,23−26] and excitation energy transfer processes[12,27−29] in the RC.

Recently, Fleming and co-workers have studied the electronic coherence dynamics in the RC using a two-color photon echo experiment and suggested that correlated excitation energy fluctuation caused by the protein environment plays an important role in preserving electronic coherence in photosynthetic complexes.[6] Thus, it is desirable to perform a detailed theoretical investigation on the electronic−vibrational couplings and their correlations in the RC.

Theoretical models for the electronic−vibrational couplings were developed to study the spectroscopic features and energy transfer dynamics of the RC. These studies were based on fitting the experimental results[30,31] or molecular dynamics simulations.[32−34] Accurate calculation of transition energy and its coupling to intra- and intermolecular motions of large molecules is still a challenging task, while there are steady progresses in this area. Quantum chemistry calculation for excited states can now be performed on relatively large molecules using the time-dependent density functional theory (TDDFT) to obtain the

Received: October 4, 2011
Revised: December 19, 2011
Published: December 21, 2011

transition frequencies and the intramolecular electronic−vibrational couplings.[35−37] Regarding the coupling of electronic transitions to the protein environment, a widely used method is to perform quantum chemistry calculations for the chromopores embedded in the protein−pigment complexes, by treating the protein environment as fixed partial charges.[38−42] Usually a large number of calculations were performed on different structures generated by molecular dynamics (MD) simulation. The computational costs usually limit the quantum chemistry calculation to configuration interaction singles (CIS) methods or semiempirical methods such as Zerner's intermediate neglect of differential orbital with parameters for spectroscopic properties (ZINDO/S),[38−42] although we note that Aspuru-Guzik and co-workers have recently performed TDDFT calculations over a large number of structures from the MD trajectory[43] to investigate excitation energy fluctuation and quantum coherence in the Fenna−Matthews−Olson (FMO) complex. This is in principle more accurate than the CIS and ZINDO/S calculations but computationally more expensive.

A simpler but also widely used approach is the electrochromic shift method, where the excitation energy shifts are treated as an empirical function of the environmental electric field, which has been used widely in the study of electron transfer dynamics.[44,45] In calculating the transition energy shifts due to the environmental electric field, different forms of the couplings schemes were used, such as the dipole and partial charge coupling methods.[33,41,46,47] Recently, Renger and co-workers have used the partial charge coupling method to calculate the site energy shifts in the FMO complex,[48] as well as photosystem I,[49,50] and found good agreement with the experiment.

In this paper, we apply quantum chemistry calculations and molecular dynamics simulations to investigate the electronic−vibrational couplings in the Q_y states of the B and H pigments in the RC of *Rb. sphaeroides*. The potential energy surface shifts between the ground and Q_y states of isolated BChl *a* and BPhe molecules and the Huang−Rhys factors are calculated using DFT and TDDFT calculations. ZINDO/S calculations are then combined with MD simulations to calculate the transition energy fluctuations to obtain the spectral density due to the coupling to the protein environment. The difference between our calculation and several previous studies is that the ZINDO/S-MD calculation is used only to calculate the environmental effects on the transition energy shifts. As a computationally more efficient alternative, we have also performed calculations based on the partial charge coupling method and compared the results with the ZINDO/S-MD ones. The absorption spectra are also calculated and compared with experimental results, from which the magnitudes of inhomogeneous broadening are obtained.

This paper is organized as follows. Theory and computational details are described in Section II. In Section III, we present the calculated Huang−Rhys factors for the Q_y transition of BChl *a* and BPhe and compare them with experimental results. The spectral densities calculated from the ZINDO/S-MD and partial charge coupling methods are also presented, and the absorption spectra of B and H pigments are simulated. Conclusions and discussions are presented in Section IV.

II. THEORY AND COMPUTATIONAL DETAILS

A. Model Hamiltonian. The displaced harmonic oscillator model[25,31,51,52] is used to describe the electronic−vibrational coupling in the ground and excited states for a chromophore, where the ground and excited state Hamiltonians are written as

$$H_g = \sum_{j=1}^{N_1}\left(\frac{p_j^2}{2m_j} + \frac{1}{2}m_j\omega_j^2 q_j^2\right) + \sum_{j=1}^{N_2}\left(\frac{P_j^2}{2M_j} + \frac{1}{2}M_j\Omega_j^2 Q_j^2\right) \quad (1a)$$

$$H_e = \sum_{j=1}^{N_1}\left[\frac{p_j^2}{2m_j} + \frac{1}{2}m_j\omega_j^2(q_j - d_j)^2\right] + \sum_{j=1}^{N_2}\left[\frac{P_j^2}{2M_j} + \frac{1}{2}M_j\Omega_j^2\left(Q_j - \frac{C_j}{M_j\Omega_j^2}\right)^2\right] + E_e \quad (1b)$$

In the above eqs 1a and 1b, N_1 and N_2 are the number of intramolecular and intermolecular vibrational modes; $\{q_j,p_j, m_j,\omega_j\}$ and $\{Q_j,P_j,M_j,\Omega_j\}$ are the coordinates, momenta, masses, and frequencies of these modes; and $\{d_j\}$ and $\{C_j/M_j\Omega_j^2\}$ describe the shifts between the excited and ground state equilibrium structures. Equation 1 thus separates the total electronic−vibrational coupling into the intramolecular and intermolecular contributions. The coupling to the intramolecular vibrational modes is characterized by their individual vibrational frequency ω_j and the associated Huang−Rhys factor $S_j = d_j^2 m_j\omega_j/2\hbar$. The intermolecular coupling to the environmental degrees of freedom is described using the spectral density $J(\omega)$ defined as

$$J(\omega) = \frac{\pi}{2}\sum_{j=1}^{N_2}\frac{C_j^2}{M_j\Omega_j}\delta(\omega - \Omega_j) \quad (2)$$

We note that unlike the case of electron transfer reactions, the environmental contribution to the reorganization energy for a neutrally excited state is much smaller. It is possible that the intramolecular electronic−vibrational couplings are comparable to or even larger than the pigment−environmental interactions, such that using a model Hamiltonian in eq 1 to separate the intra- and intermolecular contributions can give a better understanding of the total electronic−vibrational coupling.

B. Quantum Chemistry Calculation. Quantum chemistry calculations were used to obtain the parameters in eqs 1a and 1b for the intramolecular vibrational modes. First, geometry optimization of isolated BChl *a* and BPhe molecules in the ground state were carried out using the Gaussian 03 program package,[53] using DFT with the B3LYP functional[54,55] and the 6-31G* basis set. For the excited state, TDDFT was applied in the Gaussian 03 package to calculate the vertical excitation energies and the oscillator strength for the pigments. TDDFT calculations using the same functional and basis set were performed with the TURBOMOLE 5.10 package,[56,57] where the EGRADE module was used to calculate the analytic energy gradients and Hessian.[58] The Huang−Rhys factors were calculated from the results of TURBOMOLE using the Dushin program,[59] which is based on curvilinear coordinates and can be used to calculate normal-mode-projected displacements for large molecules. The intramolecular reorganization energy can be obtained by summing up

contributions from each vibrational mode

$$\lambda_{\text{intra}} = \sum_{i=1}^{N_1} \lambda_i = \sum_{i=1}^{N_1} \hbar\omega_i S_i \tag{3}$$

C. Calculation of the Spectral Density. To characterize the pigment−protein coupling, time-dependent fluctuations of the instantaneous transition energies were first calculated based on a trajectory obtained from classical MD simulation. The spectral density $J(\omega)$ was then obtained through the Wiener−Khinchin theorem.[60,61] In the literature, this method has been widely used in calculating the spectral density for electron transfer reactions[44,62,63] and excited state spectra.[38,41−43]

Two different methods were used to calculate the instantaneous transition energies from the MD trajectory. The first method is similar to those used by Kleinekathöfer and co-workers,[38,41,42] where ZINDO/S calculations were performed by treating the protein and solvent environment as fixed partial charges. An important difference between this work and these previous studies[38,41,42] is that the ZINDO/S calculation is only used to calculate the environmental shifts of the transition energy but not the energy fluctuation caused by the structural fluctuations of the pigment itself. This is done by defining

$$\Delta E(t) = E_{\text{emb}}(t) - E_{\text{iso}}(t) \tag{4}$$

where E_{env} and E_{gas} are the ZINDO/S transition energies calculated for the pigment embedded in the protein environment and the isolated pigment, respectively. The advantage of such treatment is that this can to a large extent avoid the possible overestimation of reorganization energies due to the mismatch between the equilibrium ground-state MD structure and the ground-state QM structure.[64]

The second method is based on a partial charge coupling scheme similar to that used by Renger and co-workers.[48,49] In this method, the transition energy shifts are expressed as the sum of Coulomb interactions between excited and ground state partial charge differences and the environmental electric field. More specifically, the site energy shift of the pigment is calculated as follows

$$\Delta E = \frac{1}{4\pi\varepsilon_0} \sum_{I=1}^{N} \sum_{J=1}^{M} \frac{\Delta q_I \cdot q_J^{(\text{env})}}{|r_I - r_J^{(\text{env})}|} \tag{5}$$

where Δq_I is the difference between excited and ground states partial charge for the Ith atom of the pigment; $\{q_J^{(\text{env})}\}$ is the partial charges of the protein and solvent environment; N is the total number of partial charges in the pigment; M is the total number of the environment partial charges; and $|r_I - r_J^{(\text{env})}|$ is the distance between the Ith atom of the pigment and the Jth atom in the environment. No effective dielectric constant was used for electrostatic screening since we have employed an all-atom model for the Coulomb interactions.

After the time-dependent instantaneous transition energy fluctuations $\{\Delta E(t)\}$ were obtained from classical MD trajectory using either eq 4 or eq 5, $J(\omega)$ was calculated as follows:[65] A sin transform of $\Delta E(t)$ is first performed

$$A_n = \frac{2}{\tau}\int_0^\tau \sin\left(\frac{n\pi}{\tau}t\right)\Delta E(t)\mathrm{d}t \tag{6}$$

where τ is the total simulation time. The spectral density $J(\omega)$ is then calculated as

$$J(\omega)\Delta\omega = \frac{\pi\beta\omega}{2} \sum_{\omega < \pi n/\tau < \omega + \Delta\omega} \frac{1}{2}\langle A_n^2\rangle \tag{7}$$

where $\beta = 1/k_{\text{B}}T$. The reorganization energy due to intermolecular electronic−vibrational coupling (i.e., the external reorganization energy) is given by

$$\lambda_{\text{ext}} = \frac{1}{\pi}\int_0^\infty \mathrm{d}\omega \frac{J(\omega)}{\omega} \tag{8}$$

The autocorrelation function $C(t) = \langle\delta E(t)\delta E(0)\rangle$ ($\delta E(t) \equiv \Delta E(t) - \langle\Delta E\rangle$) is related to $J(\omega)$ through the Wiener−Khinchin theorem

$$C(t) = \frac{2}{\pi\beta}\int_0^\infty \frac{J(\omega)}{\omega}\cos\omega t\mathrm{d}\omega \tag{9}$$

D. Absorption Spectra. The absorption spectra for the displaced harmonic oscillator model in eq 1 can be calculated using the Fermi golden rule[25,51,52]

$$\alpha(\omega) = \frac{2\pi\omega}{3n(\omega)\hbar c}\mu_{\text{eg}}^2\int_{-\infty}^{+\infty}\mathrm{d}t\,\exp[it(\omega_{\text{eg}} - \omega) - \gamma_{\text{e}}|t|/2]C_1(t)C_2(t) \tag{10}$$

In the above equation, ω_{eg} is the electronic transition frequency; $n(\omega)$ is the refractive index at frequency ω; γ_{e} is the rate constant of excited state population relaxation; and μ_{eg} denotes the electronic transition dipole moment. The correlation functions $C_1(t)$ and $C_2(t)$ contain contributions from the intramolecular and intermolecular vibrational modes

$$C_1(t) = \exp[-\sum_{j=1}^{N_1} S_j\{(2\bar{n}_j + 1) - (\bar{n}_j + 1)e^{i\omega_j t} - \bar{n}_j e^{-i\omega_j t}\}] \tag{11}$$

where $\bar{n}_j = (e^{\hbar\omega_j/k_{\text{B}}T} - 1)^{-1}$ and

$$C_2(t) = \exp\left\{\frac{1}{\pi}\int_0^\infty J(\omega)/\omega^2[\coth(\beta\hbar\omega/2)[\cos(\omega t) - 1] + i(\sin\omega t)]\right\} \tag{12}$$

It should be noted that the static disorder causes inhomogeneous broadening to the absorption spectra. This term is included by a convolution of the above spectra with a Gaussian function defined as

$$G(\omega) = \frac{1}{\sigma\sqrt{2\pi}}\exp[-\omega^2/2\sigma^2] \tag{13}$$

The full width at half-maximum (fwhm) of the Gaussian distribution is $2(2\ \ln\ 2)^{1/2}\sigma$. Currently, the inhomogeneous broadening terms caused by static disorder can not be treated effectively using simulation methods due to the limitation of simulation time scales and are often obtained by fitting to the experimental spectra.

III. RESULTS

A. Quantum Chemistry Calculation. The phytyl tails of the BChl *a* and BPhe molecules were replaced by methyl groups in the DFT and TDDFT calculations to reduce the computational costs,

Table 1. Huang−Rhys Factors and Reorganization Energies of the BChl *a* and BPhe Molecules through Quantum Chemistry Calculation[a]

BChl *a*						BPhe					
ω	S	λ	ω	S	λ	ω	S	λ	ω	S	λ
189	0.013	2.4	1181	0.0021	2.5	119	0.020	2.4	915	0.0021	1.9
211	0.017	3.6	1195	0.0033	3.9	144	0.0079	1.1	1088	0.0010	1.0
572	0.0019	1.1	1200	0.0062	7.4	153	0.013	2.0	1136	0.0038	4.3
639	0.0039	2.5	1207	0.0012	1.5	183	0.017	3.1	1155	0.0010	1.0
714	0.0029	2.1	1216	0.0019	2.3	351	0.0034	1.2	1169	0.0016	1.9
753	0.0081	6.1	1225	0.0017	2.0	636	0.0053	3.4	1220	0.0016	2.0
772	0.0029	2.2	1231	0.0015	1.8	716	0.0016	1.1	1233	0.0032	4.0
779	0.0037	2.9	1262	0.0040	5.0	726	0.0015	1.1	1237	0.0016	2.0
810	0.0026	2.1	1348	0.0055	7.4	754	0.0046	3.5	1252	0.0012	1.4
860	0.0048	4.1	1381	0.0031	4.3	767	0.0038	2.9	1257	0.0020	2.5
903	0.0023	2.1	1390	0.0020	2.8	808	0.0028	2.3	1267	0.0032	4.1
1093	0.0021	2.3	1436	0.0013	1.9	822	0.0019	1.5	1385	0.0037	5.1

[a] Units for ω and λ are cm^{-1}. Only the vibrational modes with $\lambda > 1$ cm^{-1} are included.

which should have little influence on the transition properties.[66−68] The calculated transition energies of the Q_y states for BChl *a* and BPhe in the gas phase using the TD-B3LYP method are 1.84 and 1.93 eV, respectively. These values are higher than the experimental results[13] by about 0.2 eV, which is consistent with a previous calculation of the BChl *a* and BPhe transition energies.[37] This is also consistent with the typical mean absolute deviation of 0.2−0.3 eV obtained with the most accurate functionals in TDDFT for singlet excited states.[69,70] The difference between the excitation energies of BChl *a* and BPhe is 0.09 eV, which agrees well with the experimental result of 0.1 eV.[12]

Normal mode analyses for the ground and excited states were performed using the Turbomole 5.10 program,[56,57] and the dushin program[59] is used to calculate the Huang−Rhys factors. The calculated Huang−Rhys factors and reorganization energies for the BChl *a* and BPhe in the gas phase were listed in Table 1, where only vibrational modes with $\lambda_i > 1$ cm^{-1} are listed. In the literature, the Huang−Rhys factors for BChl *a* have been determined from experimental studies using resonance Raman spectra,[13,16] hole-burning spectra,[14,15] or fluorescence line narrowing[17,18] methods. The experimental vibrational frequencies and Huang−Rhys factors from ref 13 were plotted in Figure 1(a) and compared with the calculated results in Figure 1(b). It can be seen that the calculated vibrational frequencies and Huang−Rhys factors agree reasonably well with the experimental ones. The total reorganization energy for BChl *a* from the quantum chemistry calculation is 132 cm^{-1}, while the experimental result from resonance Raman spectra in buffered detergent solution (Lauryl dimethyl amino oxide, LDAO) is around 200 cm^{-1}.[13] Several peaks in the 250−450 cm^{-1} range are missing in the gas-phase results but are present in the intermolecular couplings represented in $J(\omega)$ (see Figure 5(a)), so these peaks are probably due to coupling to the protein environment. The calculated results for BPhe were also given in Figure 1(c), which show a structure similar to the BChl *a*. The calculated reorganization energy from the intramolecular vibrational modes for BPhe is 122 cm^{-1}. We note that in a recent work[18] Rätsep et al. have performed similar TDDFT calculations on the

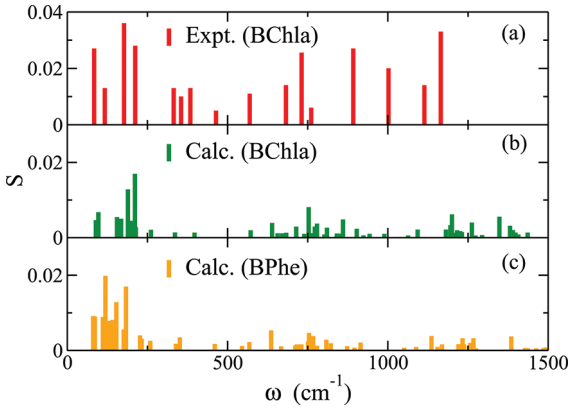

Figure 1. Huang−Rhys factors for isolated BChl *a* and BPhe molecules. (a) Experimental results from resonance Raman spectra.[13] (b) Calculated results for BChl *a*. (c) Calculated results for BPhe.

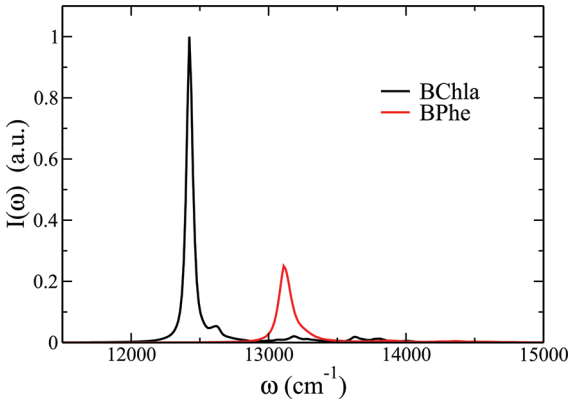

Figure 2. Calculated absorption spectra for isolated BChl *a* and BPhe molecules at 77 K.

electronic−vibrational coupling in the BChl *a* molecule and compared them to a wide range of experimental results in different solvents and temperatures from the recent resonant Raman scattering and hole-burning studies.[16,18,71] They have also considered a range of quantum chemistry calculation methods and found that the long-range corrected density functional CAM-B3LYP may give slightly better results than the B3LYP functional when comparing to those experiments.[18]

The gas-phase absorption spectra at 77 K for BChl *a* and BPhe molecules are calculated using eq 11 by setting $C_2(t) = 1$ and plotted in Figure 2. The lifetimes of the BChl *a* and BPhe excited states, which are caused primarily by excitation energy transfer from H to B and from B to P, are taken as 150 and 100 fs, respectively.[6] The excitation energies of the BChl *a* and BPhe molecules are shifted to their corresponding experimental values. The small peaks around 13 200 cm^{-1} for BChl *a* and 13 900 cm^{-1} for BPhe are due to vibrational progression. Obviously, the gas-phase spectra are significantly narrower than the experimental spectra (see Figure 7) due to the neglect of the pigment−protein couplings.

B. Combined MD and ZINDO/S Calculation. The RC of purple bacteria *Rb. sphaeroides* was simulated using the NAMD program.[72] The structure of the RC protein−pigment complex was first retrieved from the Protein Data Bank (code: 1PCR).[73] Lauryl dimethyl amino oxide (LDAO) molecules were added

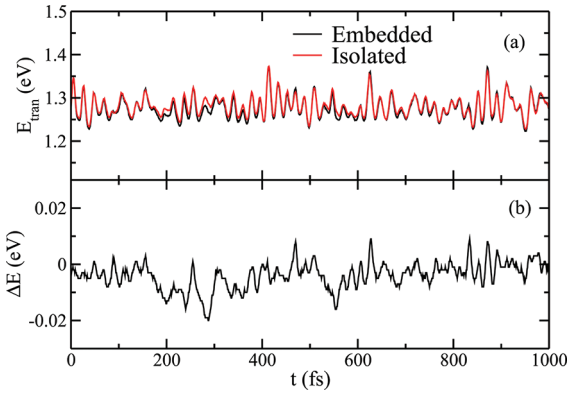

Figure 3. Transition energies calculated with the ZINDO/S method: (a) For the pigment embedded in the protein environment and the isolated pigment. (b) Their differences as defined in eq 4.

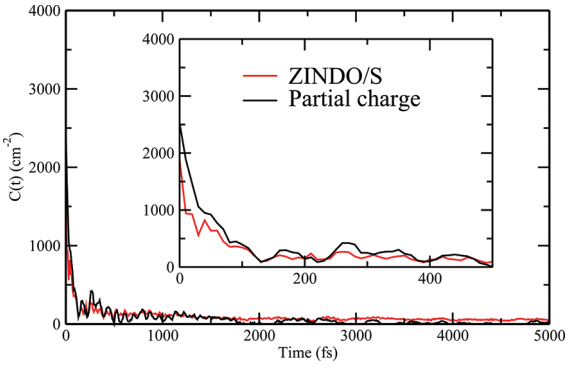

Figure 4. Correlation function of excitation energy fluctuations for the B_M pigment at 77 K, calculated using the ZINDO/S method and partial charge coupling method.

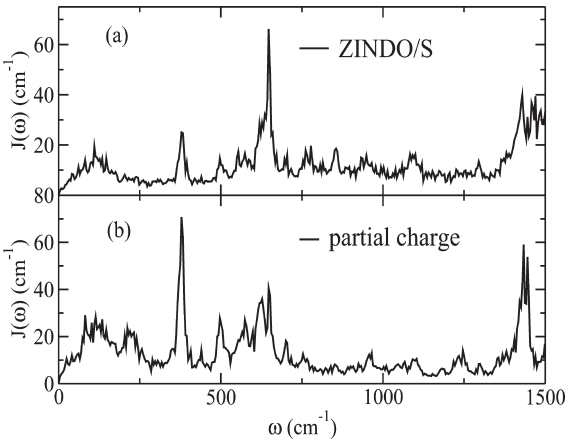

Figure 5. Spectral density calculated for the B_M pigment, calculated using the ZINDO/S method and partial charge coupling method.

around the protein to provide an effective hydrophobic environment as described in ref 74. Finally, the LDAO and RC system were hydrated with TIP3P water, and Na^+ and Cl^- ions were added to the system to simulate an ionic concentration of 0.15 M. The total system contains 81 595 atoms, including 20 166 water molecules (160 of them were crystallographic), 160 LDAO molecules (9 of them were crystallographic), 78 Na^+ ions, 73 Cl^- ions, and one RC complex. The CHARMM27 force field[75] was used in the simulation. For the force field of the cofactors B, P, and H, the parameters from Floppe et al.[76] and partial charges from Ishikita et al.[32] were used. The force field parameters for LDAO were fitted following the scheme described in ref 77. The final system was first minimized and equilibrated for 100 ps at 10 K, then slowly heated to 77 K, and equilibrated at this temperature for 5 ns before collecting the trajectory for further ZINDO/S calculations. The simulation time step is 1 fs.

Very often, a continuum of time scales exist in the sluggish protein environment. It is thus difficult for trajectories of a few nanoseconds to characterize the slow components of the excitation energy fluctuations. In this study, the slowest fluctuation included was up to a 100 ps time scale. This is done by truncating a MD trajectory into a few 100 ps segments and averaging the results over them.[78] Longer time fluctuations that are not captured in this method can be treated as static disorder. To this end, a total number of six trajectories, each with the length of 100 ps, are used in the calculation of the correlation functions and spectral density. The MD structures are recorded every 10 fs during the simulation, making each trajectory segment contain 10 000 frames for analyzing.

The ORCA program[79] was used to calculate the transition energy from the ground states to the Q_y states for BChl *a* and BPhe. To improve the efficiency of the ZINDO calculations, the pythyl tails of the pigments were replaced by H atoms. All the atoms surrounding the target pigment were treated as point charges. Figure 3(a) shows the transition energies of BChl *a* in the L site of the RC at 77 K. The two curves show the time-dependent transition energy fluctuations for the pigment embedded in the protein environment (the black line) and in the gas phase (the red line). We can see that these two curves look very similar except for small differences. The reason for the similarity is that the intramolecular vibrational modes contribute most to the transition energy fluctuations from the ZINDO/S calculations.

The reorganization energy calculated directly from the transition energy fluctuations is around 400 cm^{-1}, which is much larger than that calculated using TDDFT in Section III.A. The major reason for the overestimation of reorganization energies is due to the mismatch between the equilibrium ground-state MD and QM structures:[64] In the combined MD and ZINDO/S calculations, the transition energies are calculated close to the equilibrium structure of the classical force field, which are biased from the quantum chemistry equilibrium structure. This may lead to distorted energy fluctuations and overestimate the fluctuations of transition energies caused by intramolecular vibrational modes. As stated in Section I, to avoid the errors caused by the structure mismatch between the classical force field and quantum chemistry calculation, we have focused on the environmental effects only, by subtraction of the gas-phase transition energies from those calculated with the protein and solvent environment. As shown in Figure 3(b), the calculated $\Delta E(t)$ shows much smaller fluctuations.

The autocorrelation function calculated from the time series $\Delta E(t)$ is shown in Figure 4. The majority of the correlation function decays within 100 fs. The calculated spectral density of BChl *a* is shown in Figure 5. By comparing with Figure 1, we can see that some of the peaks in $J(\omega)$, such as those near 650 and 1400 cm^{-1}, are due to intramolecular vibrational modes. There is a continuous distribution of frequencies lower than 200 cm^{-1},

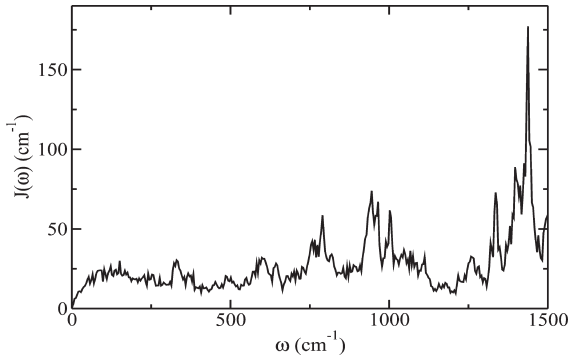

Figure 6. Spectral density calculated for the H_M pigment.

Table 2. Reorganization Energies of the Four B and H Pigments Calculated Using the ZINDO/S and Partial Charge Coupling Methods[a]

	ZINDO/S	partial charge
B_M	17.6 (0.8)	23.6 (0.4)
B_L	16.0 (0.6)	16.8 (0.3)
H_M	39.5 (0.6)	
H_L	50.5 (3.3)	

[a] Unit is cm^{-1}. Numbers in the parentheses are standard deviations.

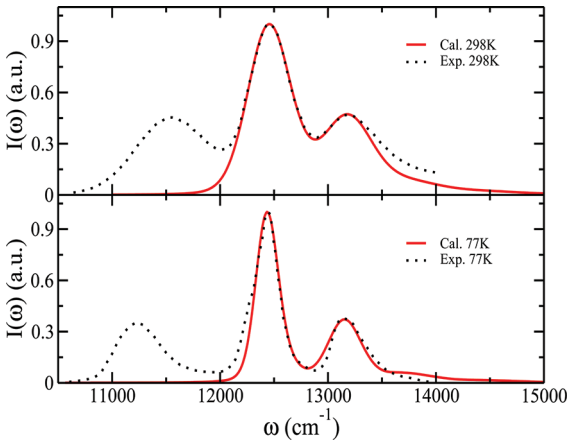

Figure 7. Simulated absorption spectra for BChl *a* and BPhe at 77 and 298 K, in comparison with experiment results.

which are caused by the pigment−protein interaction. The spectral density of BPhe is shown in Figure 6. Finally, the calculated reorganization energies from eq 8 for the four B and H pigments are given in Table 2.

In calculating the absorption spectra, the B(H) pigments associated with the two different subunits M and L are treated identically since the difference between the averaged ΔE values for the two pigments is rather small. For example, the $\langle \Delta E \rangle$ values are -47 ± 5 and -24 ± 7 cm^{-1} for the B_M and B_L pigments, respectively. The difference between them is much smaller than the inhomogeneous broadening terms needed to reproduce the experimental spectra (see below).

The calculated absorption spectra at 77 and 298 K are shown in Figure 7 and compared with the experimental spectra.[13] Inhomogeneous broadening with fwhm of 210 cm^{-1} for BChl *a* at 77 K, 210 cm^{-1} for BPhe at 77 K, 410 cm^{-1} for BChl *a* at 298 K, and 430 cm^{-1} for BPhe at 298 K was added in the calculation. The calculated absorption line shapes agree well with those from the experiment.[13] From these values, we can see that there is still a large portion of the pigment−protein coupling that is not captured by the ZINDO/S-MD calculations.

An interesting question concerning the pigment−protein coupling is that recent experiment has suggested a strong correlation between the energy gap fluctuations of the B and H pigments.[6] We have thus also calculated the cross-correlation between different chromophores using the ZINDO/S data. The cross-correlation between each pair of the four pigments B_L, B_M, H_L, and H_M was calculated, and no obvious evidence for strong couplings between two different pigments was found.

C. Partial Charge Coupling Method. In this subsection, we use the partial charge coupling method described in eq 5 to calculate the fluctuation of transition energies for the Bchl *a* pigments. The partial charge differences Δq_I were taken from ref 46 by Renger and co-workers. The autocorrelation function $C(t)$ and spectral density $J(\omega)$ are then calculated and compared with the ZINDO/S results in Figures 4 and 5. It can be seen that the autocorrelation function and spectral density calculated using the partial charge coupling method and the ZINDO/S method are very similar. The reorganization energies for the B_M and B_L pigments are given in Table 2, which are also close to the ZINDO/S results. As the partial charge coupling method is much simpler than the ZINDO/S calculations, we conclude that it can be a good alternative to model the pigment−protein coupling.

IV. CONCLUSIONS AND DISCUSSIONS

The paper has combined quantum chemistry calculation and MD simulation to investigate the electronic−vibrational coupling in the Q_y excited states of BChl *a* and BPhe pigments in the RC of *Rb. sphaeroides*. Quantum chemistry calculations were employed to obtain the Huang−Rhys factors for the isolated pigment molecules using the displaced-harmonic oscillator model. The results compare reasonably well with experiments from the Resonance Raman studies,[13] as well as the recent experimental and theoretical studies on difference fluorescence narrowing spectra for BChl *a*.[18] We have also calculated the electronic−vibrational coupling to the protein environment by combining MD simulation with the ZINDO/S and partial charge coupling methods. The spectral densities were obtained by analyzing the time-dependent transition energy fluctuations. Finally, the calculated Huang−Rhys factors and spectral densities were used to simulate the absorption spectra of the B and H pigments, and the magnitude of inhomogeneous broadening was obtained by comparing with the experimental spectra.

In our ZINDO/S-MD calculation, we have adopted a different approach from several previous works.[38,41,43] Namely, since we have separated the intra- and intermolecular contributions to the total electronic−vibrational coupling, the former can now be calculated using more accurate quantum chemistry methods, while the ZINDO/S calculations were used only to calculate excitation energy fluctuations caused by the protein environment. In this way, we can avoid to a large extent the errors caused by the mismatch between equilibrium structures from the classical force field and quantum chemistry calculations, as such a mismatch may lead to an overestimation of the transition energy fluctuations caused by intramolecular vibrational modes.

However, the problem is not solved completely, and the current treatments have neglected the mechanic distortion of the equilibrium pigment structure in the protein environment due to short-range interactions. This should lead to an underestimation of excitation energy shifts. Thus, more consistent theoretical methods to treat the structural fluctuations and their influence on excitation energy fluctuations are still needed. The ZINDO/S-MD results were also compared with those from the partial charge coupling method. It is shown that carefully fitted partial charge differences can give reliable results in modeling the pigment−protein coupling.

As stated in Section I, an important motivation of this paper is trying to find the correlations in transition energy fluctuations between the B and H pigments observed in the recent experiment.[6] So far, this question can only be partially answered: First, it is reasonable to assume that the excitation energy fluctuations caused by the intramolecular vibrational modes should not be correlated. Second, the ZINDO/S-MD calculations have shown little correlation between the B and H pigments within the time scale of our MD simulation. However, since the reorganization energies from the ZINDO/S-MD calculation are rather small (20−50 cm^{-1}), a large portion of the pigment−protein coupling that is slow and not captured in the MD simulation is treated as static disorder with fwhm's around 200−300 cm^{-1} at 77 K and 400 cm^{-1} at 298 K. Because of the simulation time scales, not much can be said about whether these static disorder terms are correlated or not. Thus, further experimental and theoretical studies are needed to resolve the problem.

AUTHOR INFORMATION

Corresponding Author

*E-mail: qshi@iccas.ac.cn.

ACKNOWLEDGMENT

The authors would like to thank Prof. J. Smith and Prof. N. Foloppe for the kind help with the force field. Part of the computational work was done at the Supercomputer Center of the Chinese Academy of Sciences (SCCAS). This work is supported by NSFC (Grant No. 91027015), the 973 program (Grant No. 2011CB808502), and the Chinese Academy of Sciences (Grant No. KJCX2.YW.H17 and the Hundred Talents Project).

REFERENCES

(1) *Molecular Mechanisms of Photosynthesis*; Blankenship, R. E., Ed.; Blackwell Science: London, 2000.
(2) Ke, B. *Photosynthesis: photobiochemistry and photobiophysics*; Springer: Netherlands, 2001.
(3) Deisenhofer, J.; Epp, O.; Miki, K.; Huber, R.; Michel, H. *J. Mol. Biol.* **1984**, *180*, 385–398.
(4) Allen, J.; Williams, J. *FEBS Lett.* **1998**, *438*, 5–9.
(5) Reimers, J.; Hush, N. *J. Chem. Phys.* **2003**, *119*, 3262.
(6) Lee, H.; Cheng, Y.-C.; Fleming, G. R. *Science* **2007**, *316*, 1462.
(7) Aartsma, T.; Matysik, J. *Biophysical techniques in photosynthesis*; Springer Verlag: Dordrecht, The Netherlands, 2008.
(8) Hunter, C.; Daldal, F.; Thurnauer, M. *The purple phototrophic bacteria*; Springer Verlag: Dordrecht, The Netherlands, 2008.
(9) Zinth, W.; Wachtveitl, J. *Chem. Phys. Chem.* **2005**, *6*, 871–880.
(10) Jennings, R.; Zucchelli, G.; Croce, R.; Valkunas, L.; Finzi, L.; Garlaschi, F. *Photosynth. Res.* **1997**, *52*, 245–253.
(11) Yang, M.; Damjanovic, A.; Vaswani, H.; Fleming, G. *Biophys. J.* **2003**, *85*, 140–158.
(12) Parkinson, D.; Lee, H.; Fleming, G. *J. Phys. Chem. B* **2007**, *111*, 7449–7456.
(13) Cherepy, N.; Shreve, A.; Moore, L.; Boxer, S.; Mathies, R. *J. Phys. Chem. B* **1997**, *101*, 3250–3260.
(14) Reddy, N.; Picorel, R.; Small, G. *J. Phys. Chem.* **1992**, *96*, 6458–6464.
(15) Lyle, P.; Kolaczkowski, S.; Small, G. *J. Phys. Chem.* **1993**, *97*, 6924–6933.
(16) Frolov, D.; Gall, A.; Lutz, M.; Robert, B. *J. Phys. Chem. A* **2002**, *106*, 3605–3613.
(17) Wendling, M.; Pullerits, T.; Przyjalgowski, M.; Vulto, S.; Aartsma, T.; Grondelle, R. V.; Amerongen, H. V. *J. Phys. Chem. B* **2000**, *104*, 5825–5831.
(18) Rätsep, M.; Cai, Z.; Reimers, J.; Freiberg, A. *J. Chem. Phys.* **2011**, *134*, 024506.
(19) Vos, M.; Rappaport, F.; Lambry, J.; Breton, J.; Martin, J. *Nature* **1993**, *363*, 320–325.
(20) Pullerits, T.; Visscher, K.; Hess, S.; Sundström, V.; Freiberg, A.; Timpmann, K.; Van Grondelle, R. *Biophys. J.* **1994**, *66*, 236–248.
(21) Shelly, K.; Carson, E.; Beck, W. *J. Am. Chem. Soc.* **2003**, *125*, 11810–11811.
(22) Sugisaki, M.; Fujii, R.; Cogdell, R.; Hashimoto, H. *Photosynth. Res.* **2008**, *95*, 309–316.
(23) Jortner, J. *J. Am. Chem. Soc.* **1980**, *102*, 6676–6686.
(24) Zharikov, A.; Scherer, P.; Fischer, S. *J. Phys. Chem.* **1994**, *98*, 3424–3431.
(25) Lin, S. H.; Chang, C. H.; Liang, K. K.; Chang, R.; Shiu, Y. J.; Zhang, J. M.; Yang, T.-S.; Hayashi, M.; Hsu, F. C. *Adv. Chem. Phys.* **2002**, *121*, 1.
(26) Parson, W.; Warshel, A. *Chem. Phys.* **2004**, *296*, 201–216.
(27) Cheng, Y.-C.; Engel, G. S.; Fleming, G. R. *Chem. Phys.* **2007**, *341*, 285–295.
(28) Cheng, Y.; Lee, H.; Fleming, G. *J. Phys. Chem. A* **2007**, *111*, 9499–9508.
(29) Cheng, Y.-C.; Fleming, G. R. *J. Phys. Chem. A* **2008**, *112*, 4254–4260.
(30) Chang, C.; Hayashi, M.; Chang, R.; Liang, K.; Yang, T.; Lin, S. *J. Chin. Chem. Soc.* **2000**, *47*, 785–797.
(31) Lin, S.; Alden, R.; Hayashi, M.; Suzuki, S.; Murchison, H. *J. Phys. Chem.* **1993**, *97*, 12566–12573.
(32) Ishikita, H.; Loll, B.; Biesiadka, J.; Galstyan, A.; Saenger, W.; Knapp, E. *FEBS Lett.* **2005**, *579*, 712–716.
(33) Souaille, M.; Marchi, M. *J. Am. Chem. Soc.* **1997**, *119*, 3948–3958.
(34) Kosztin, I.; Schulten, K. *Biol. Technol. Photosynth.* **2008**, 445–464.
(35) Ceccarelli, M.; Lutz, M.; Marchi, M. *J. Am. Chem. Soc.* **2000**, *122*, 3532–3533.
(36) Sundholm, D. *Phys. Chem. Chem. Phys.* **2003**, *5*, 4265–4271.
(37) Muñoz-Losa, A.; Curutchet, C.; Galván, I.; Mennucci, B. *J. Chem. Phys.* **2008**, *129*, 034104.
(38) Damjanović, A.; Kosztin, I.; Kleinekathöfer, U.; Schulten, K. *Phys. Rev. E* **2002**, *65*, 31919.
(39) Vasil'ev, S.; Bruce, D. *Biophys. J.* **2006**, *90*, 3062–3073.
(40) Yin, S.; Dahlbom, M.; Canfield, P.; Hush, N.; Kobayashi, R.; Reimers, J. *J. Phys. Chem. B* **2007**, *111*, 9923–9930.
(41) Olbrich, C.; Kleinekathöfer, U. *J. Phys. Chem. B* **2010**, *114*, 12427–12437.
(42) Olbrich, C.; Jansen, T.; Liebers, J.; Aghtar, M.; Strumpfer, J.; Schulten, K.; Knoester, J.; Kleinekathöfer, U. *J. Phys. Chem. B* **2011**, *115*, 758–764.
(43) Shim, S.; Rebentrost, P.; Valleau, S.; Aspuru-Guzik, A. arXiv: 1104.2943v1, 2011.
(44) Marchi, M.; Gehlen, J.; Chandler, D.; Newton, M. *J. Am. Chem. Soc.* **1993**, *115*, 4178–4190.
(45) Gehlen, J.; Marchi, M.; Chandler, D. *Science* **1994**, *263*, 499.

(46) Adolphs, J.; Renger, T. *Biophys. J.* **2006**, *91*, 2778–2897.
(47) Mukai, K.; Abe, S.; Sumi, H. *J. Phys. Chem. B* **1999**, *103*, 6096–6102.
(48) Adolphs, J.; Muh, F.; Madjet, M. E.-A.; Renger, T. *Photosynth. Res.* **2008**, *95*, 197–209.
(49) Renger, T. *Photosynth. Res.* **2009**, *102*, 471–485.
(50) Adolphs, J.; Muh, F.; Madjet, M.; Busch, M.; Renger, T. *J. Am. Chem. Soc.* **2010**, *132*, 3331–3343.
(51) Mukamel, S. *Principles of Nonlinear Optical Spectroscopy*; Oxford University Press: Oxford, 1995.
(52) May, V.; Kühn, O. *Charge and Energy Transfer Dynamics in Molecular Systems*, 2nd ed.; Wiley-VCH: Weinheim, 2004.
(53) Frisch, M. J. et al. *Gaussian 03*, revision E.01; Gaussian, Inc.: Pittsburgh PA, 2004.
(54) Lee, C.; Yang, W.; Parr, R. *Phys. Rev. B* **1988**, *37*, 785.
(55) Becke, A. *Chem. Phys.* **1993**, *98*, 5648–5652.
(56) Deglmann, P.; Furche, F. *J. Chem. Phys.* **2002**, *117*, 9535.
(57) Deglmann, P.; Furche, F.; Ahlrichs, R. *Chem. Phys. Lett.* **2002**, *362*, 511–518.
(58) Furche, F.; Ahlrichs, R. *J. Chem. Phys.* **2002**, *117*, 7433.
(59) Reimers, J. *J. Chem. Phys.* **2001**, *115*, 9103.
(60) Wiener, N. *Acta Math.* **1930**, *55*, 117–258.
(61) Khintchine, A. *Math. Ann.* **1934**, *109*, 604–615.
(62) Ando, K. *J. Chem. Phys.* **1997**, *106*, 116.
(63) Sadygov, R.; Hao, Z.; Huhmer, A. *Anal. Chem.* **2008**, *80*, 376–386.
(64) Zwier, M.; Shorb, J.; Krueger, B. *J. Comput. Chem.* **2007**, *28*, 1572–1581.
(65) van Kampen, N. G. *Stochastic processes in physics and chemistry*; Elsevier: New York, 2007.
(66) Cory, M.; Zerner, M.; Hu, X.; Schulten, K. *J. Phys. Chem. B* **1998**, *102*, 7640–7650.
(67) Janosi, L.; Kosztin, I.; Damjanović, A. *J. Chem. Phys.* **2006**, *125*, 014903.
(68) Mercer, I.; Gould, I.; Klug, D. *J. Phys. Chem. B* **1999**, *103*, 7720–7727.
(69) Silva-Junior, M.; Schreiber, M.; Sauer, S.; Thiel, W. *J. Chem. Phys.* **2008**, *129*, 104103.
(70) Jacquemin, D.; Wathelet, V.; Perpete, E.; Adamo, C. *J. Chem. Theory Comput.* **2009**, *5*, 2420–2435.
(71) Zazubovich, V.; Tibe, I.; Small, G. *J. Phys. Chem. B* **2001**, *105*, 12410–12417.
(72) Kalé, L.; Skeel, R.; Bhandarkar, M.; Brunner, R.; Gursoy, A.; Krawetz, N.; Phillips, J.; Shinozaki, A.; Varadarajan, K.; Schulten, K. *J. Comput. Phys.* **1999**, *151*, 283–312.
(73) Ermler, U.; Fritzsch, G.; Buchanan, S.; Michel, H. *Structure* **1994**, *2*, 925–936.
(74) Ceccarelli, M.; Marchi, M. *J. Phys. Chem. B* **2003**, *107*, 1423–1431.
(75) MacKerell, A., Jr.; Bashford, D.; Bellott, M.; Dunbrack, R., Jr.; Evanseck, J.; Field, M.; Fischer, S.; Gao, J.; Guo, H.; Ha, S. *J. Phys. Chem. B* **1998**, *102*, 3586–3616.
(76) Foloppe, N.; Ferrand, M.; Breton, J.; Smith, J. *Proteins* **1995**, *22*, 226–244.
(77) Autenrieth, F.; Tajkhorshid, E.; Baudry, J.; Luthey-Schulten, Z. *J. Comput. Chem.* **2004**, *25*, 1613–1622.
(78) LeBard, D.; Matyushov, D. *J. Phys. Chem. B* **2009**, *113*, 12424–12437.
(79) Petrenko, T.; Neese, F. *J. Chem. Phys.* **2007**, *127*, 164319.